

RESEARCH ARTICLE

# Predicting anti-cancer activity of quinoline derivatives: CoMFA and CoMSIA approach

Ankur Vaidya<sup>1</sup>, Abhishek Kumar Jain<sup>1</sup>, Prashantha Kumar<sup>2</sup>, Sushil Kumar Kashaw<sup>1</sup>, and Ram Kishore Agrawal<sup>1</sup>

<sup>1</sup>Department of Pharmaceutical Sciences, Dr. Hari Singh Gour Vishwavidyalaya, Sagar, India and <sup>2</sup>Department of Pharmaceutical Sciences, JSS College of Pharmacy, Ooty, India

## Abstract

The 3D quantitative structure-activity relationships of 31 quinoline nuclei containing compounds and their biological activity have been investigated to establish various models. The comparative molecular field analysis (CoMFA) and comparative molecular similarity indices analysis (CoMSIA) studies resulted in reliable and significant computational models. The obtained CoMFA model showed high predictive ability with  $q^2=0.592$ ,  $r^2=0.966$  and standard error of estimation (SEE)=0.167, explaining majority of the variance in the data with two principal components. Predictions obtained with CoMSIA steric, electrostatic, hydrophobic, hydrogen-bond acceptor and donor fields ( $q^2=0.533$ ,  $r^2=0.985$ ) showed high prediction ability with minimum SEE (0.111) and four principal components. The information obtained from the CoMFA and CoMSIA contour maps can be utilized for the design and development of topoisomerase-II inhibitors for synthesis.

**Keywords:** QSAR, CoMFA, CoMSIA, topoisomerase, quinoline

## Introduction

Quinoline derivatives represent a large number of antiproliferative agents exhibiting cytotoxicity through DNA intercalation, causing interference in replication process.<sup>1-3</sup> Actinomycin D, doxorubicin, mitoxantrone and streptonigrin are quinoline analogs possessing antibacterial or anti-cancer activity through DNA intercalation. Most of these drugs are currently used in the treatment of human malignancies target topoisomerase (types II) enzymes.<sup>4-6</sup>

Topoisomerase inhibitors designated as “poisons” interact with DNA to form cleavable complexes, causing permanent DNA damage that triggers a series of cellular events finally inducing apoptosis or other types of cell death. There are two classes of DNA topoisomerase: (i) type I enzyme breaks one DNA strand for the passage of a second strand, (ii) type II enzyme breaks both strands of one DNA duplex for the passage of a second DNA double strand. DNA topoisomerases (types II) are the primary target for a number of pharmaceutical agents including etoposide, doxorubicin and mitoxantrone.<sup>7-9</sup>

Quantitative structure-activity relationship (QSARs) is an attempt to correlate structural features of the compounds with their *in vitro* or *in vivo* activity to design new entities with improved activity. However, the classic QSAR model is only a rough approximation to the real relationships as it mainly uses 2-D molecular descriptors.<sup>10-13</sup> Attempts have been made to incorporate comparative molecular field analysis (CoMFA) and comparative molecular similarity indices analysis (CoMSIA) techniques in 3D QSAR as powerful and versatile tools to build and design an activity model (QSAR) in rational drug design.<sup>14-17</sup> These techniques involve generation of a common three dimensional lattice around a set of molecules and calculation of interaction energies at the lattice points. In a strategy to reduce the problem of discrimination and tumour resistance we should continuously design and synthesize new compounds for the betterment of the society. In conclusion of our earlier attempt to develop predictive CoMFA and CoMSIA model for designing new

Address for Correspondence: Prof. Ram Kishore Agrawal, PhD, Department of Pharmaceutical Sciences, Dr. Hari Singh Gour Vishwavidyalaya, Sagar, India. Tel.: +91-7582- 233934. Fax: +91-7582-264236. E-mail: ramkishoreagrawal@gmail.com

(Received 24 October 2010; revised 27 January 2011; accepted 25 February 2011)

compound, here we report both CoMFA and CoMSIA of quinoline derivatives as potent anti-cancer agents using software SYBYL 6.7.

## Methods

### Data set

A data set of 31 quinoline derivatives with their topoisomerase (types II) inhibitory activity induced cytotoxicity on MCF7 cancer cell line has been taken for QSAR analysis (Table 1).<sup>18–20</sup>

### Molecular structure and alignment

Structures of the quinoline compounds were built on the workspace of Silicon Graphics work station molecular modelling software SYBYL version 6.7 (Tripos Inc. 2001).<sup>21</sup> The most active compound was built from fragments in the SYBYL fragment library, and the geometry-optimization was carried out using the standard Tripos molecular mechanics force field with a distance-dependent ( $1/r$ ) dielectric function and the Powell conjugate gradient algorithm with a convergence criterion of 0.001 kcal/mol. Partial charges for all the molecules were assigned using Gasteiger-Huckel method, and it was submitted for conformational search protocol using multi-search method with the following settings: maximum cycles 400, maximum conformers 100, energy cut-off 30 kcal/mol, number of hits 12, maximum rms gradient 3.0 and tolerance 0.40. The conformer of most active compound with the lowest energy was then used.

Alignment of molecules is the most critical step for the development of CoMFA and CoMSIA model. In the present study, quinoline derivative with the highest  $pIC_{50}$  (compound no. 1c) served as template, and all molecules were superimposed on the template via field fit alignment technique. Figure 1 shows the display of aligned molecules. Following alignment the molecules were placed within a lattice that extended 4 Å units beyond the aligned molecules in all directions with a grid step size of 2 Å, a probe  $sp^3$  hybridized carbon atom with +1 charge and Van der Waals radius of 1.52 Å was employed.

### CoMFA and CoMSIA studies

The 3D QSAR models were derived employing the CoMFA and CoMSIA method using 31 compounds in the data set. CoMFA was performed with 25 compounds in training set and 6 compounds (1f, 2b, 2h, 3c, 4b and 4j) in the test set. Test and training set contains diverse set of compounds with low, moderate and high biological activity.

In CoMFA, steric and electrostatic field descriptors were calculated with the distant-dependent dielectric constant. A default cut-off of 30 kcal/mol was used to truncate both steric and electrostatic field energies. In the CoMSIA, five force fields properties i.e. steric, electrostatic, hydrophobic, hydrogen-bond donor and

hydrogen-bond acceptor were determined for all the molecules. A 30-kcal/mol energy cut-off was applied for all five force fields, which meant that the energies fields greater than 30 kcal/mol are curtailed to that value, and thus can avoid infinity of energy values inside the molecule.

### Regression analysis

As for the modelling methods, the CoMFA and CoMSIA energies fields were used as independent variables with the  $pIC_{50}$  activity value as a dependent variable. Partial least-squares (PLS) regression analyses were conducted and cross validation was performed using leave-one-out method with 2 kcal/mol column filter. The cross-validated correlation coefficient ( $q^2$ ), was calculated using the equation.

## Results and discussion

The final model was developed with an optimum number of components ( $N$ ) yielding the highest cross-validated correlation coefficient ( $q^2$ ) to avoid overfitted 3D QSARs. The optimum number of components to be used in the model derivation was chosen from the analysis with the highest cross-validated correlation coefficient ( $q^2$ ).

### CoMFA results

CoMFA model with significant internal and external predictive ability was selected with a high  $q^2$  value of 0.592 at the optimum number of components as two. The non-cross-validated  $r^2$  (LOO) value was 0.966 with standard error of estimate (SEE) 0.167 and covariance ratio (F) 84.018 (significant at 99% level). The probability of  $r^2$  ( $P$  value) ranging to zero is zero ( $P = 0$ ) (Table 2). The correlation between experimental and predicted activity with residual activity for both training and test set of compounds are shown in Table 1 and represented graphically in Figure 2. These results authenticate the good prediction ability of the generated CoMFA model.

The CoMFA contour plots, showed the relative positions of the local fields around aligned molecules that were important for activity variation in the model. The CoMFA contour plots depict the steric and electrostatic fields of the compounds that were generated by the contribution of 81.2 and 18.8% field contribution, respectively, through PLS model (Figure 3). The larger sizes of the green–yellow polyhedra relative to the red–blue polyhedra are consistent and revealed the dominance of steric fields (81.2%) over the electrostatic field (18.8%) for these compounds. Greater values of “Bio-Activity Measurement” are correlated with more bulk near green, less bulk near yellow, more negative charge near blue and more positive charge near red. Results insist that the steric region or bulk group substitution is preferred for higher activity. A large green contour near the fourth position substituted amine

Table 1. Structures of compounds used in the study with their biological activities.

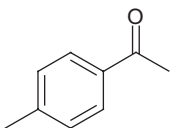
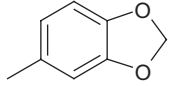
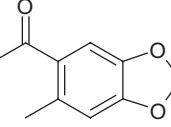
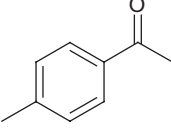
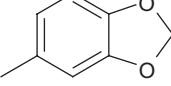
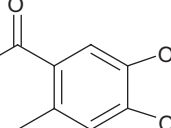
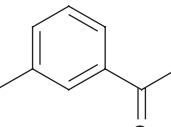
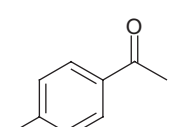
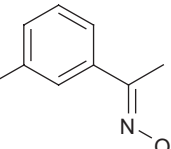
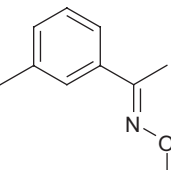
S. No.	X	Y	Z	Actual $pIC_{50}$	CoMFA predicted $pIC_{50}$	CoMFA residual	CoMSIA predicted $pIC_{50}$	CoMSIA residual
1a		Cl	7-OCH <sub>3</sub>	3.602	3.737	-0.135	3.551	0.051
1b		Cl	H	2.358	2.617	-0.259	2.554	-0.196
1c		Cl	H	4.301	4.093	0.208	4.235	0.066
1d		H	7-OCH <sub>3</sub>	3.698	3.570	0.128	3.687	0.011
1e		H	H	1.899	1.867	0.032	1.783	0.116
1f		H	H	3.552	3.101	0.451	3.200	0.352
2a		H	H	1.600	1.528	0.072	1.604	0.004
2b		H	H	2.085	2.825	-0.740	2.653	-0.568
2c		H	H	1.823	1.783	0.040	1.842	-0.019
2d		H	H	1.742	1.688	0.054	1.812	-0.070

Table 1. continued on next page

Table 1. Continued.

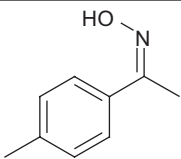
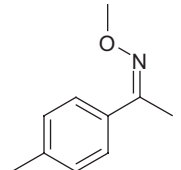
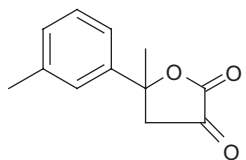
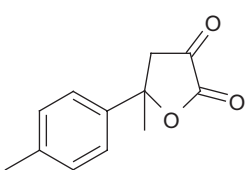
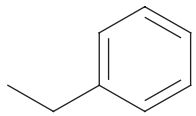
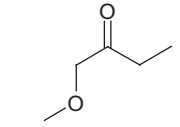
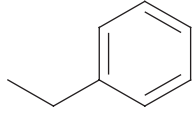
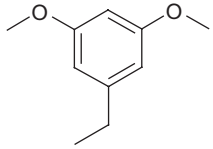
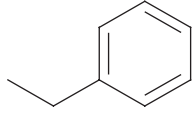
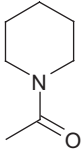
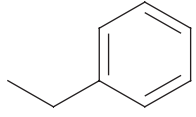
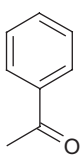
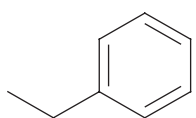
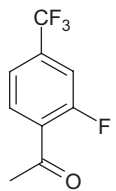
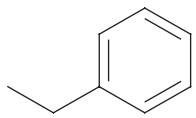
S. No.	X	Y	Z	Actual $pIC_{50}$	CoMFA predicted $pIC_{50}$	CoMFA residual	CoMSIA predicted $pIC_{50}$	CoMSIA residual
2e		H	H	2.465	2.362	0.103	2.253	0.212
2f		H	H	1.860	2.190	-0.330	2.014	-0.154
2g		H	H	2.430	2.406	0.024	2.348	0.082
2h		H	H	2.480	2.588	-0.108	2.758	-0.278
3a	H		H	2.207	2.077	0.130	2.258	-0.051
3b			H	1.481	1.579	-0.098	1.563	-0.082
3c			H	1.327	1.927	-0.600	1.827	-0.500
3d			H	1.853	1.847	-0.006	1.901	-0.048
3e			H	1.886	1.787	0.099	1.885	0.001
3f			H	1.886	2.013	-0.127	1.760	0.126

Table 1. continued on next page

Table 1. Continued.

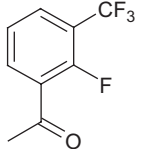
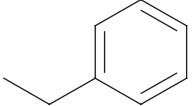
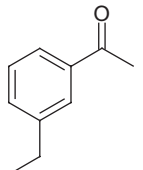
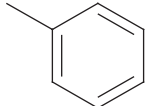
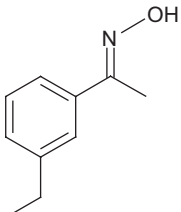
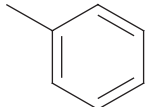
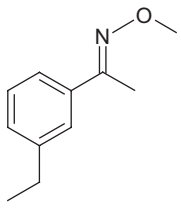
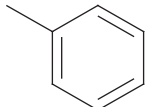
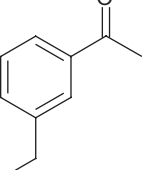
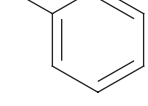
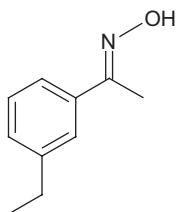
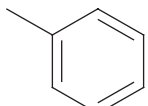
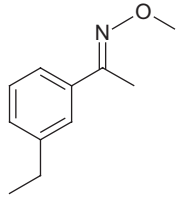
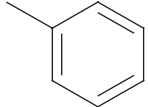
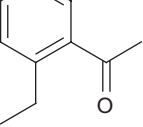
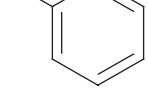
S. No.	X	Y	Z	Actual $pIC_{50}$	CoMFA predicted $pIC_{50}$	CoMFA residual	CoMSIA predicted $pIC_{50}$	CoMSIA residual
3g			H	1.721	1.673	0.048	1.744	-0.023
4a			6-OCH <sub>3</sub>	2.607	2.573	0.034	2.619	-0.012
4b			6-OCH <sub>3</sub>	2.832	2.766	0.066	2.925	-0.093
4c			6-OCH <sub>3</sub>	2.300	2.327	-0.027	2.311	-0.011
4d			8-OCH <sub>3</sub>	1.266	1.128	0.138	1.130	0.136
4e			8-OCH <sub>3</sub>	2.159	2.509	-0.350	2.294	-0.135
4f			8-OCH <sub>3</sub>	2.712	2.618	0.094	2.674	0.038
4g			8-OCH <sub>3</sub>	2.732	2.620	0.112	2.747	-0.015

Table 1. continued on next page

Table 1. Continued.

S. No.	X	Y	Z	Actual $pIC_{50}$	CoMFA predicted $pIC_{50}$	CoMFA residual	CoMSIA predicted $pIC_{50}$	CoMSIA residual
4h			8-OCH <sub>3</sub>	3.420	3.358	0.062	3.349	0.071
4i			8-H	3.455	3.524	-0.069	3.556	-0.101
4j			8-OCH <sub>3</sub>	1.625	1.944	-0.319	1.895	-0.270

Reproduced with copyright permission from American Chemical Society and Elsevier.

(X substitution) of quinoline ring, indicates that the bulky substitution favours the activity. The presence of bulky group like 1-(benzo[d][1,3]dioxol-5-yl)ethanone at 4th position substitution (compound 1c) is conducive for activity. Naturally, 1-(benzo[d][1,3]dioxol-5-yl)ethanone is more bulky in the series, while acetophenone is less at 4th position thus compound 1c is more active than 1a. The activity may further be enhanced by substituting some bulkier group like propyl, isopropyl or long chain alkyl at 1-(benzo[d][1,3]dioxol-5-yl)ethanone. The yellow contour above the furan ring system (Y substitution) leads to cause less steric contribution. Thus the presence of small group substitution or unsubstitution (such as the presence of H in compound 1d) enhances the biological activity. Similarly, blue contour on top of the furan ring substitution, indicates that substitution with electronegative groups like CN, F, Cl increase the activity (Cl in compounds 1a and 1c). Electropositive substitution demonstrated with red contour has no significant contribution in activity.

### CoMSIA results

For selected CoMSIA model, the cross-validated  $r^2$  ( $q^2$ ) value of the training set was 0.533 with four principal components. The non-cross-validated  $r^2$  value was 0.985 with an SEE of 0.111 and a covariance ratio (F) of 194.806 (significant at the 99% level). The field fit alignment of the quinoline derivatives and the correlation between the experimental activity (EA) and the calculated activity (PA) are shown in Figures 1 and 4, respectively. These results reveal the good prediction ability of generated model. Supplementary data clearly illustrate the steric, electrostatic, hydrogen-bond donor, hydrogen-bond acceptor and hydrophobic field interaction in the CoMSIA model. In the CoMSIA

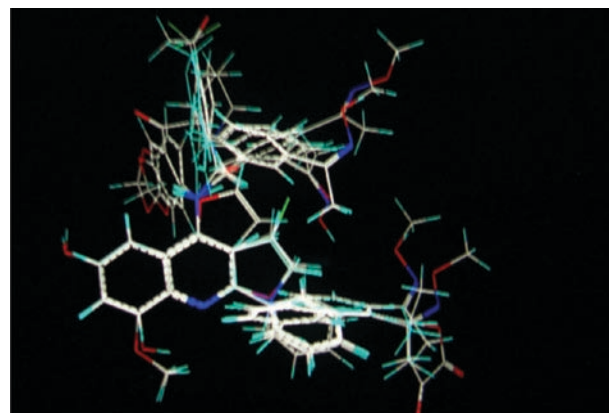


Figure 1. Field fit alignment of quinoline derivatives.

Table 2. The comparison of PLS statistics results of 3D QSAR models of CoMFA and CoMSIA.

PLS statistics	CoMFA	CoMSIA
PCs	2	4
$r^2$	0.966	0.985
$q^2$	0.592	0.533
SEE	0.167	0.111
F value	84.018	194.806
P value	0.0	0.0
<i>Field Contribution</i>		
Steric	0.812	0.271
Electrostatic	0.188	0.092
Hydrophobicity		0.319
H bond acceptor		0.130
H bond donor		0.187

model, the contributions of the steric, electrostatic, hydrophobic, hydrogen-bond acceptor and hydrogen-bond donor fields were 31.1, 16.2, 40.9, 03.1, and 08.7%, respectively (Table 2), and represented graphically in



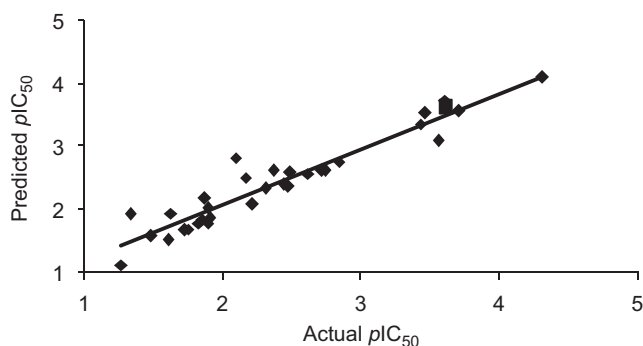


Figure 2. Correlation between the experimental and predicted activities of the developed CoMFA model.

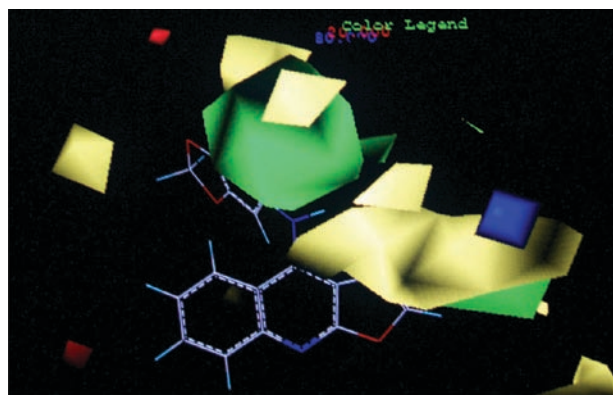


Figure 3. CoMFA contour plots for steric and electrostatic regions. Green counters indicate the bulky group region, whereas yellow counter indicates region where bulky groups are not required. Blue counters indicate the region needed electronegative contribution, whereas red counters indicate the region where electropositive contribution required.

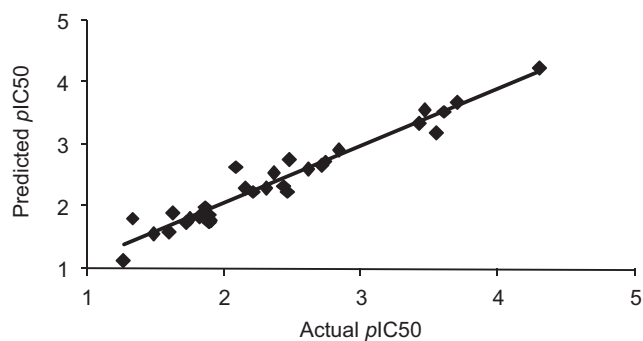


Figure 4. Correlation between the experimental and predicted activities of the developed CoMSIA model.

Figure 5. The contour maps of generated fields are shown in Figure 5. Similar to CoMFA, the presence of green contour near the fourth amine substituted quinoline derivatives indicated that the bulky groups (i.e. 1-(benzo[d][1,3]dioxol-5-yl)ethanone) at this position increased activity (X substitution; compound 1c). The

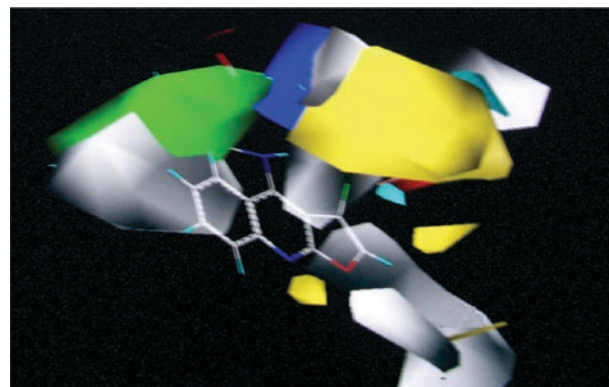


Figure 5. CoMSIA contour plots. Green counters indicate the bulky group region, whereas yellow counter indicate region where bulky groups are not required. Blue counters indicate the region needed electronegative contribution, whereas red counters indicate the region where electropositive contribution required. The white contour near suggest that hydrophobic groups will increase activity. The purple and orange contour for both hydrogen-bond donor favour and not favour, respectively, in biological activity. Similarly contour for both hydrogen-bond acceptor favour and disfavour are showed by magenta contour and red contour, respectively.

yellow contour above the furan ring system indicates that bulky substituents at this position decrease anti-cancer activity (Y substitution) and small group substitution or unsubstitution (i.e. H in compound 1d) enhance the biological activity. The blue contour above the furan ring indicates that the biological activity will increase by an electronegative group at the aforementioned positions (i.e. presence of Cl in compounds 1a and 1c). The insignificant red region points to electropositive substitutions specify no significant changes in biological activity. In the hydrophobic contour plots, the white contour near 5th, 6th and 7th positions of quinoline ring and the 1st, 2nd and 3rd positions of furan ring system suggest that hydrophobic groups like long chain alkyls at this position will increase activity (compound 1d). The purple and orange contours for both hydrogen-bond donor favoured and not favoured are absent showing no contribution in biological activity. Similarly, contours for both hydrogen-bond acceptor favoured and disfavoured (magenta contour and red contour, respectively) showed no contribution in anti-cancer activity.

## Conclusion

In conclusion, current QSAR studies have established a reliable 3D QSAR (CoMFA and CoMSIA) models. The developed models, significant and reliable, indicate the importance of substitution at respective positions for anti-cancer activity, which can efficiently guide further modification of quinoline analogs to obtain more potent anti-cancer quinoline derivatives.

## Declaration of interest

The authors report no conflict of interest.

## References

- Ryckebusch A, Garcin D, Lansiaux A, Goossens JF, Baldeyrou B, Houssin R et al. Synthesis, cytotoxicity, DNA interaction, and topoisomerase II inhibition properties of novel indeno[2,1-c]quinolin-7-one and indeno[1,2-c]isoquinolin-5,11-dione derivatives. *J Med Chem* 2008;51:3617-3629.
- Ferlin MG, Chiarello G, Gasparotto V, Dalla Via L, Pezzi V, Barzon L et al. Synthesis and *in vitro* and *in vivo* antitumor activity of 2-phenylpyrroloquinolin-4-ones. *J Med Chem* 2005;48:3417-3427.
- Gasparotto V, Castagliuolo I, Chiarello G, Pezzi V, Montanaro D, Brun P et al. Synthesis and biological activity of 7-phenyl-6,9-dihydro-3H-pyrrolo[3,2-f]quinolin-9-ones: A new class of antimitotic agents devoid of aromatase activity. *J Med Chem* 2006;49:1910-1915.
- Pommier Y. DNA topoisomerase I and II in cancer chemotherapy: Update and perspectives. *Cancer Chemother Pharmacol* 1993;32:103-108.
- Bhargava R, Lal P, Chen B. HER-2/neu and topoisomerase II $\alpha$  gene amplification and protein expression in invasive breast carcinomas: Chromogenic *in situ* hybridization and immunohistochemical analyses. *Am J Clin Pathol* 2005;123:889-895.
- Schmidt F, Knobbe CB, Frank B, Wolburg H, Weller M. The topoisomerase II inhibitor, genistein, induces G2/M arrest and apoptosis in human malignant glioma cell lines. *Oncol Rep* 2008;19:1061-1066.
- Lucio VBD, Marina VM, Rodriguez RB. The molecular biology of topoisomerase II $\alpha$  and its importance in the acquisition of multidrug resistance in cancer. *Clin. Transl Oncol* 2002;4:170-178.
- Staker BL, Hjerrild K, Feese MD, Behnke CA, Burgin AB Jr, Stewart L. The mechanism of topoisomerase I poisoning by a camptothecin analog. *Proc Natl Acad Sci USA* 2002;99:15387-15392.
- Duguet M. When helicase and topoisomerase meet! *J Cell Sci* 1997;110 (Pt 12):1345-1350.
- Ravichandran V, Jain PK, Mourya VK, Agrawal RK. QSAR study on some arylsulfonamides as anti-HIV agents. *Med Chem Res* 2007;16:342-351.
- Ravichandran V, Mourya VK, Agrawal RK. QSAR Study of novel 1,1,3-trioxo [1,2,4]-thiadiazine (TTDs) analogues as potent anti-HIV agents. *ARKIVOC* 2007;14:204-212.
- Ravichandran V, Mourya VK, Agrawal RK. QSAR Modeling of HIV-1 Reverse transcriptase inhibitory activity with PETT derivatives. *Dig J Nanomat Biostr* 2008;3:9-17.
- Ravichandran V, Mourya VK, Agrawal RK. QSAR Analysis of 6-aryl-2,4-dioxo-5-hexenoic acids as HIV-1 integrase inhibitors. *Ind J Phar Edu Res* 2008;42:40-47.
- Ravichandran V, Agrawal RK. Predicting anti-HIV activity of PETT derivatives: CoMFA approach. *Bioorg Med Chem Lett* 2007;17:2197-2202.
- Ravichandran V, Sankar S, Agrawal RK. Comparative molecular similarity indices analysis for predicting anti-HIV activity of phenyl ethyl thiourea (PET) derivatives. *Med Chem Res* 2008;17:1-11.
- Prashantha Kumar BR, Sankar G, Nasir Baig RB, Chandrashekar S. Novel Biginelli dihydropyrimidines with potential anticancer activity: A parallel synthesis and CoMSIA study. *Eur J Med Chem* 2009;44:4192-4198.
- Prashanthakumar BR, Nanjan MJ. Comparative molecular similarity indices analysis for predicting the antihyperglycemic activity of thioglitazones. *Med Chem Res* 2010;19:1000-1010.
- Chen YL, Chen IL, Wang TC, Han CH, Tzeng CC. Synthesis and anticancer evaluation of certain 4-anilino-furo[2,3-b]quinoline and 4-anilino-furo[3,2-c]quinoline derivatives. *Eur J Med Chem* 2005;40:928-934.
- Lee BD, Li Z, French KJ, Zhuang Y, Xia Z, Smith CD. Synthesis and evaluation of dihydropyrroloquinolines that selectively antagonize P-glycoprotein. *J Med Chem* 2004;47:1413-1422.
- Chen YL, Huang CJ, Huang ZY, Tseng CH, Chang FS, Yang SH et al. Synthesis and antiproliferative evaluation of certain 4-anilino-8-methoxy-2-phenylquinoline and 4-anilino-8-hydroxy-2-phenylquinoline derivatives. *Bioorg Med Chem* 2006;14:3098-3105.
- SYBYL [computer program], version 6.7. St. Louis (MO): Tripose Associates, USA.